Sensors and Actuators B 222 (2016) 71–77

Contents lists available at ScienceDirect

Sensors and Actuators B: Chemical

journal homepage: www.elsevier.com/locate/snb

Electrochemical surface plasmon resonance sensing with absorptive redox mediator film

Sergiy Patskovsky*, Anne-Marie Dallaire, Michel Meunier

Department of Engineering Physics, Laser Processing and Plasmonics Laboratory, Polytechnique, Montréal, P.O. 6079, Station Centre-ville, QC, H3C 3A7, Canada

ARTICLE INFO

Article history:
Received 2 June 2015
Received in revised form 21 July 2015
Accepted 11 August 2015
Available online 14 August 2015

Keywords:
Surface plasmon resonance
Electrochemical sensors
Redox tags
Stem-loop oligonucleotides

ABSTRACT

Surface plasmon resonance (SPR) spectroscopy has been used for the detection of reversible refractive index changes that occur in a redox mediator film during potentiostatic oxydoreduction. We investigated the theoretical and experimental parameters of electrochemical SPR (eSPR) sensing using as an example of the electroactive labels the Methylene Blue (MB) organic dye. The optimal eSPR interrogation method for MB sensing in a solution and in a uniform interfacial thin film formed by stem-loop oligonucleotides tagged with MB are evaluated. Electrochemical activation of the optical SPR response depends on the local MB concentration and can be used to design sensitive and highly selective biosensing approaches.

1. Introduction

Continuous, sensitive and real-time analysis of complex, unprocessed aqueous samples is an essential requirement for a broad spectrum of biosensing applications ranging from medical diagnostics to environmental monitoring. Even though many of the current biosensor technologies show exquisite sensitivities and limits of detection in laboratory settings, their use in point-of-care applications is still impeded by a high level of nonspecific response in crude samples due to the confounding effects of non-specific adsorption to sensor surface [1]. One of the potential solutions to this challenge is to combine compatible biosensing approaches into one analytical tool that is able to measure and analyze a higher quantity of complementary parameters. In this article, we consider such an analytical tool based on the integration of electrochemical and surface plasmon resonance (SPR) sensing methods.

The electrochemical transducers offer a very attractive low-cost approach for converting the results of biochemical events into a measurable analytical signal. The most common transduction principle is based on the detection of faradaic current generated by electroactive redox mediators. A good example of such redox mediator is methylene blue (MB), an organic dye that has been applied as an electron transfer mediator [2] and as an electrochemical indicator for oligonucleotides hybridization [3,4]. Due to the relative scarceness of electroactive contaminants in biological samples, MB can be used as a very selective redox tag and has already shown great performance for analyte detection in complex media when integrated into E-DNA structure switching sensors [5,6]. Electrochemical transduction can also be achieved with the spectral analysis of a MB mediator film: the red-absorbing oxidized state of MB can be converted to its reduced, colorless leuco-MB state using potentiostatic reduction. Spectroelectrochemical analysis of this phenomenon was experimentally realized with an optical waveguide platform [7,8]. On the other hand, SPR is recognized as one of the most sensitive analytical tool for the optical detection of biological binding at an interface and is widely used for biosensing and bio-affinity measurements. In an effort to further enhance its versatility and sensitivity, SPR has been integrated with electrochemistry, which allows to gain a new insight into the changes in optical properties occurring as a result of electrochemical phenomena. This integrated electrochemical SPR device (eSPR) has notably been used for the characterization of electropolymerized thin films [9–14] and for the monitoring of refractive index changes in a redox mediator film during bio-recognition processes [15–18]. In the last years, the eSPR technique has led to exciting results by measuring the electrochemical modulation of redox tags with a plasmonic sensor [19–22]. Recently, we presented an example of such sensor based on electrochemical structure-switching sensors adapted for the SPR detection method [23]. In this approach, we immobilized a stem-loop DNA probe modified with a MB tag on a gold plasmonic electrode. Upon hybridization of the target, the stem-loop unfolds and changes the distance between the

* Corresponding author.
E-mail address: sergiy.patskovsky@polymtl.ca (S. Patskovsky).

http://dx.doi.org/10.1016/j.snb.2015.08.051
0925-4005/

redox-active MB reporter and the gold, thus changing its electron transfer efficiency. We activated the redox activity of MB using electrochemistry and then measured the resulting changes in refractive index with SPR. We found this method to be highly selective even in complex media and adaptable in a multiplexed format.

However, we believe that a more detailed investigation of the combined eSPR transducing principle for redox mediators sensing is necessary. Indeed, an important effect that is often overlooked in the eSPR literature is the difference in absorption between the oxidized and reduced states of the mediator, as is the case for MB. The theoretical aspects of absorption-based SPR principle were previously investigated [24] and employed for the detection of ammonium ions, the development of a SPR enzyme sensor [25] and for probing of absorptive nanoplasmonic particles attached to a gold substrate [26]. In this work, we aim to define the optimal parameters of experimental eSPR technique applied for and fully realize potential of electroactive SPR biosensing in selectivity, sensitivity and eventual eSPR analytical tool construction. enhance the detection sensitivity of thin films of various compositions and various properties, notably absorbing films [27]. We think that such eSPR technique is a promising technology to overcome the problem of limited selectivity and nonspecific responses of biosensors in real complex liquids.

2. Materials and methods

2.1. Materials

Methylene blue powder, Tris(carboxyethyl)phosphine (TCEP), Phosphate buffered saline (PBS 10 mM, pH 7.2) and all other reagents were obtained from Sigma–Aldrich. Oligonucleotides were purchased from Biosearch Technologies (Petaluma, CA). Stem-loop oligonucleotide P2 (5′ HS-MC6-act ctc caa gcg ccg act gtt gag agg-MB 3′) contains a sequence complementary to the rpoB gene of Mycobacterium Tuberculosis associated with drug resistant tuberculosis. It was modified at its 5′ end with a thiol group to promote immobilization to the gold surface and at its 3′ end with a methylene blue (MB) reporter. This oligonucleotide was designed to adopt a stem-loop conformation with a 5 base pairs stem.

2.2. Structure-switching sensor film preparation

Prior to functionalization, glass slides with 50 nm thin gold film were cleaned by an oxygen plasma cleaner, rinsed in MilliQ water and dried under a N_2 flow. Stem-loop oligonucleotides were immobilized on the sensor surface with thiol-gold chemistry (Fig. 1(II)) using the following protocol. First, to reduce disulfide bonds between the thiol-modified oligonucleotides, 2 μL of 100 μM P2 were incubated with 4 μL of 10 mM reducing agent TCEP for an hour at 4 °C. This mix was then diluted in 350 μL PBS to obtain a P2 concentration of 650 nM. Second, a 175 μL drop of this solution was placed on the gold chip and left to incubate for an hour in a humid chamber at room temperature. Third, the chip was rinsed with water and incubated in a solution of 2 mM 6-mercapto-1-hexanol (MCH) in PBS at 4 °C overnight. MCH fills the free sites on the gold using thiol-gold chemistry and has three functions: passivate the electrode, block non-specific adsorption and maintain the oligonucleotides in an upright orientation. As the stem-loop oligonucleotides P2 maintain the MB molecules near the electrode, this functionalization protocol effectively results in a single layer of MB at a fixed distance from the surface.

3. Experimental electrochemical SPR system

To perform synchronous measurements of electrochemical voltammograms and conventional SPR spectroscopy, we designed the multi-parametric experimental platform presented in Fig. 1. A white light source (LED, Thorlabs), collimating optics and a BK7 Dove coupling prism were used for SPR excitation in the Kretschmann configuration over a 50 nm gold film. This metal film was used as a working electrode (3 mm diameter disk) in a three-electrode configuration and the electrochemical experiments were controlled by a potentiostat (Solartron ModuLab). A platinum disk (1 cm diameter) and an Ag/AgCl electrode filled with 3 M KCl electrolyte were used respectively as a counter-electrode and as a reference electrode. Upon application of a voltage scan on the gold film, the SPR spectrum at a fixed incident angle was analyzed in real-time by a custom-written *LabView* software. To find and monitor the SPR resonance peak position and its amplitude, dynamic tracking centroid algorithms [28] were applied. A plastic measuring open-cell with a capacity of 5 mL was designed and the liquid was agitated at constant speed with a mechanical stirrer (Instech) during experiments. Two types of samples were characterized: the first was a solution of MB in PBS, resulting in an absorbing media with dye molecules free to diffuse (Fig. 1(I)), the second was a PBS buffer media and a surface functionalized with P2 oligonucleotides that fix the MB molecules close to the electrode, resulting in an absorbing interfacial layer (Fig. 1(II)).

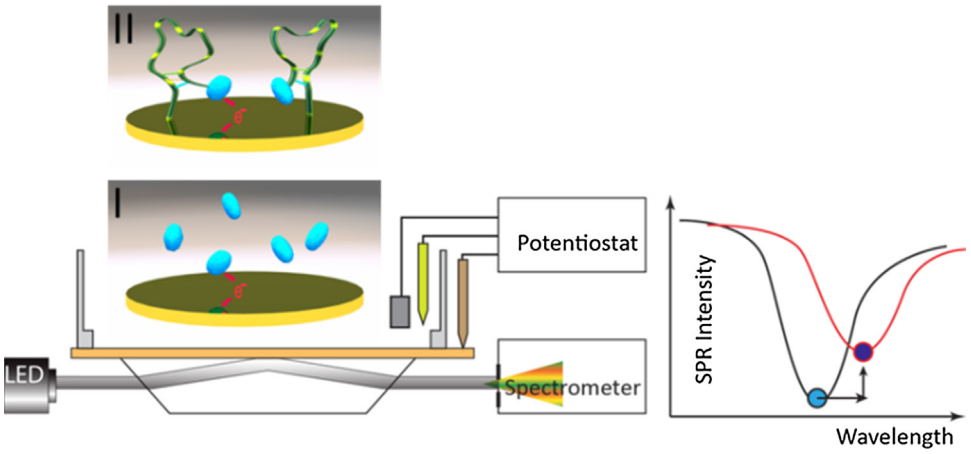

Fig. 1. Schematic of the electrochemical SPR experimental system with spectral interrogation method. A collimated white light is sent at a fixed angle on the SPR chip through a dove prism and analyzed with a spectrometer to obtain the resonant wavelength and intensity of the SPR spectral curve. The gold chip is simultaneously used as the working electrode in an electrochemical cell. Two types of redox-active media were tested: (I) MB in solution and (II) Stem-loop oligonucleotides with MB redox tag.

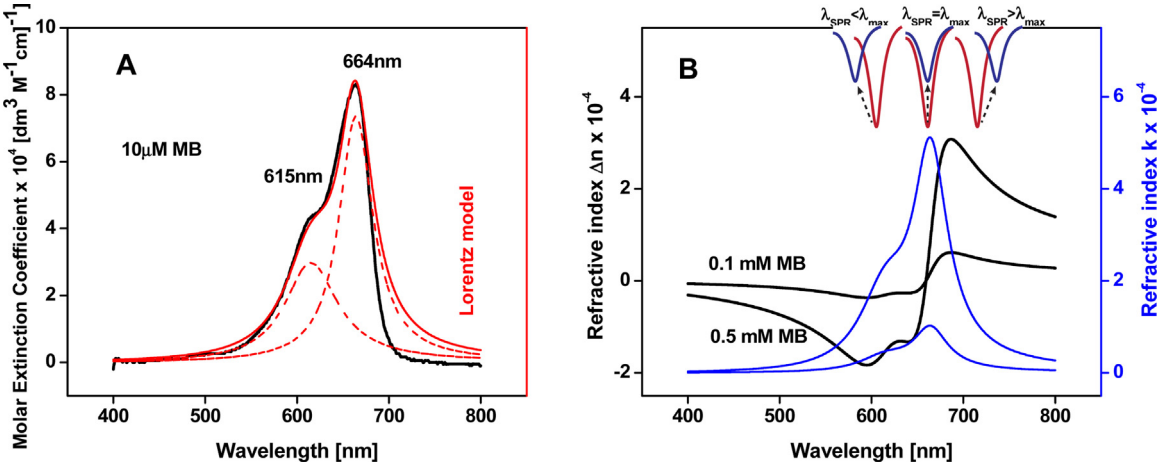

Fig. 2. Optical properties of the oxidized state of methylene blue dye and their influence on the SPR spectral peak. (A) Experimental absorption extinction coefficient of 10 μM MB (black) and the corresponding Lorentz model for two oscillators resonant at 615 and 664 nm (red). (B) Theoretical complex refractive index (real part n: black, imaginary part k: blue) calculated from the two-oscillators Lorentz model for solutions of 0.1 mM and 0.5 mM MB in water. (Inset) Influence of the MB optical properties on the SPR peak shift as a function of the SPR spectral position (λ_{SPR}) relative to the MB absorption peak (λ_{max}). (For interpretation of the references to color in this figure legend, the reader is referred to the web version of the article.)

4. Results and discussion

In regards to the refractive index of the analyzed medium, a conventional SPR sensor measures only changes in the real part associated with the peak resonant wavelength. In the case of a sensing layer containing absorbing markers such as MB dye, changes in both the real and imaginary parts that result from the optical absorption have to be monitored. This was experimentally realized by detecting both the SPR resonance peak position and amplitude in optical-absorption-based SPR sensors [24]. To theoretically estimate the properties of SPR sensors with spectral interrogation for optical absorption detection, we applied the Fresnel equation for multilayer structure. Three or four layer were considered including the BK7 coupling prism, plasmon supporting thin gold film in direct contact with the absorbing medium (i.e. MB solution) or with the absorbing interfacial layer in a buffer medium (i.e. MB-modified oligonucleotides). The dielectric constant ε_s of the MB absorbing layer that consists of N_{MB} absorbing oscillators per unit volume can be obtained by assuming a Lorentz model:

$$\varepsilon_s = \varepsilon_s^{\infty} + N_{MB}\left(\frac{e^2}{m_e\varepsilon_0}\right)\left(\frac{f}{\omega_0^2-\omega^2-i\omega\gamma}+\frac{f}{\omega 1_0^2-\omega^2-i\omega\gamma 1}\right);$$

$$\omega_0=\frac{2\pi c}{\lambda_{max}};\quad \gamma=\frac{2\pi c\lambda_{1/2}}{\lambda_{max}^2} \qquad (1)$$

where e is the elementary electric charge; m_e is the mass of an electron; ε_0 is the permittivity of vacuum; ω_0 and are the absorption frequency and the damping frequency, respectively; f is the oscillator strength, λ_s^{∞} is the background dielectric constant of the sensing layer; λ_{max} is the absorption maximum wavelength and the $\lambda_{1/2}$ is full width wavelength at half-maximum of absorption spectrum. The experimental absorption spectrum of a 10 μM MB solution is shown in Fig. 2A and was used for comparison with the theoretical spectrum calculated using Eq. (1). For the theoretical Lorentz model, we used a resonance at λ_{max} = 664 nm with $\lambda_{1/2}$ = 45 nm and an oscillator force f of 0.68 [29]. There is a shoulder on the pure MB monomer spectra at approximately λ_{max} = 615 nm which has been identified as a vibrational component of a single electronic band. This position is also very close to the resonance absorption of the MB dimer, but in our case we use a rather diluted MB solution consisting mostly of MB monomers. For the 615 nm peak, we used in the calculation $\lambda_{1/2}$ = 70 nm, f1 = 0.5 and λ_s^{∞} assumed at $(1.333)^2$, which is typical for dye molecules in water [24]. The theoretical molar extinction coefficient is obtained from the imaginary part of the refractive index that is defined by $n_s + ik_s = \sqrt{\varepsilon_s}$ and we found that the experimental results for 10 μM MB solution were well-matched with the parameters used in Eq. (1) (Fig. 2A). We also show the theoretical real and imaginary parts of the refractive index n_s and n_k of MB solutions in Fig. 2B 0.1 mM and 0.5 mM concentration. We observe that MB absorption produces nil, negative or positive variation in the real part of the RI of the sensing layer depending on the spectral position. As a result, the experimental spectral SPR curves will be shifted in different directions depending on the resonance wavelength (Fig. 2B, inset). Such particularities of absorption-based SPR sensing must be included into the analysis to correctly interpret obtained experimental SPR results.

Absorption-based SPR also employs resonance peak intensity as a sensing parameter. However, the peak intensity depends not only on absorption but also on the coupling prism RI and, most importantly, on the plasmon supporting gold layer thickness. For example, using MB as a model, we calculated spectral SPR dependences for different gold layers thickness 40 nm, 50 nm and 65 nm, and for different MB concentrations 0.1 mM, 0.2 mM and 1 mM. In Fig. 3A, we observe minimal SPR intensity variation at 50 nm gold thickness in regards to MB concentration, whereas for 40 nm and 65 nm, there are significant changes in the intensity amplitude going in opposite directions as the MB concentration is increased. In the inset of Fig. 3A, the absolute SPR intensity dependence on the gold film thickness for different MB concentrations is presented. These results confirm the importance of gold thickness optimization for efficient electrochemical SPR sensing. Using the equation for SPR resonance peak dependence [24], we obtained the differential dR_{min}/dAbs (Abs is a parameter proportional to n_s) at the resonant 664 nm spectral position. Two extremes are obtained (Fig. 3B): thinner gold layer of about 36 nm is related to negative SPR intensity variations as absorption is increased while thicker 68 nm leads to a positive SPR intensity variation. A gold thickness of about 51 nm minimizes R_{min} at 664 nm and shows the smallest overall intensity variation as absorption is varied (Fig. 3A). The following analytical equation allows us to estimate optimal gold thickness at different spectral ranges and for different SPR experimental techniques:

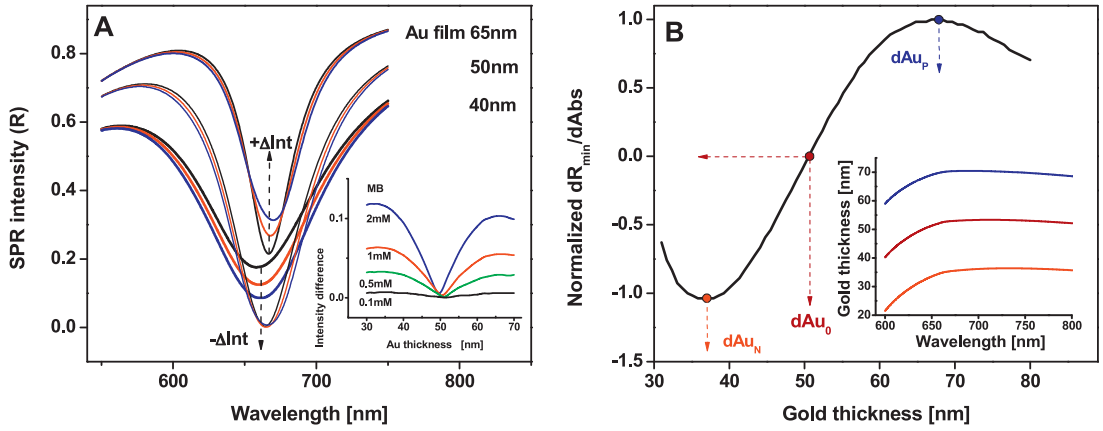

Fig. 3. (A) Spectral SPR curves at MB resonance wavelength ($\lambda_{SPR} = \lambda_{max}$) for different MB concentrations (black = 0.1 mM, red = 1 mM, blue = 2 mM) and gold layer thickness (40, 50, 65 nm). The influence of gold film thickness on the SPR intensity response to variations in MB concentration is shown. The intensity variation upon addition of MB is positive (+ΔInt) at 65 nm thickness and negative (−ΔInt) at 40 nm. (Inset) Absolute SPR intensity dependence on the gold film thickness for different MB concentrations. (B) Differential $dR_{min}/d\mathrm{Abs}$ as function of gold film thickness. R_{min} is the SPR intensity at resonance and Abs is a parameter proportional to n_s, the real part of the refractive index of MB. The gold thickness can be optimized to obtain the highest SPR intensity contrast (positive at $d\mathrm{Au_P}$, negative at $d\mathrm{Au_N}$, nil at $d\mathrm{Au_0}$) between absence and presence of the absorbing MB dye. (Inset) Spectral dependences of optimal gold thicknesses for maximal $d\mathrm{Au_N}$, $d\mathrm{Au_P}$ and minimal $d\mathrm{Au_0}$ intensity variation. (For interpretation of the references to color in this figure legend, the reader is referred to the web version of the article.)

$$d_{\mathrm{Au}} = \frac{\lambda\sqrt{\left|\varepsilon'_{\mathrm{m}}\right|}\left(\ln\left(\left|\varepsilon'_{\mathrm{m}}\right|\sin\varphi/\varepsilon''_{\mathrm{m}}\right)+K\right)}{2\pi\left(\varepsilon_{\mathrm{s}}^2+2\left|\varepsilon'_{\mathrm{m}}\right|\right)} \text{ with } \tan\frac{\phi}{2} \cong \frac{\varepsilon_{\mathrm{p}}}{\sqrt{\left|\varepsilon'_{\mathrm{m}}\right|\left(\varepsilon_{\mathrm{p}}-\varepsilon_{\mathrm{s}}\right)-\varepsilon_{\mathrm{p}}\varepsilon_{\mathrm{s}}}} \quad (2)$$

where d_{Au} is the gold layer thickness, λ is the pumping wavelength, ε_{m} and ε_{p} are the dielectric constants of the metal and coupling prism. Parameter K for $d\mathrm{Au_N} = 0.069$; for $d\mathrm{Au_0} = 2.703$, and for $d\mathrm{Au_P} = 1.386$, and the corresponding spectral dependences are shown in Fig. 3B, inset.

The real part of the absorbing media RI affects the spectral position of the SPR resonance peak. In Fig. 4 we present theoretical spectral SPR resonance curves obtained with optimal gold layer thickness 47 nm, 50 nm and 51 nm for surface plasmon excitation at 630 nm, 664 nm and 685 nm respectively. Such optimal gold thickness is equal to the optimal thickness for conventional SPR that assures close to zero reflectance at SPR resonance and is calculated using Eq. (2). Calculations are performed for water, 0.1 mM and 0.2 mM MB solutions. The absolute value of RI variation in response to the MB concentration is determined by the initial spectral position of the SPR resonance minimum in water (Fig. 2B). It is approaching maximum at 685 nm corresponding to the $\lambda_{max} + \lambda_{1/2}$ wavelength (Fig. 4). At $\lambda_{max} - \lambda_{1/2}$ we expect lower absolute RI changes as MB second absorption peak at 615 nm decreases RI variation. An increased gold film absorption at $\lambda_2 < 600$ nm also reduces the overall SPR efficiency at shorter wavelengths. We can conclude that a 685 nm excitation wavelength is optimal for detection of the real part of RI of a MB solution in a condition of using correct gold film thickness. For comparison, the dotted line in Fig. 4 shows spectral dependences of the absolute real part of RI changes for 0.5 mM MB.

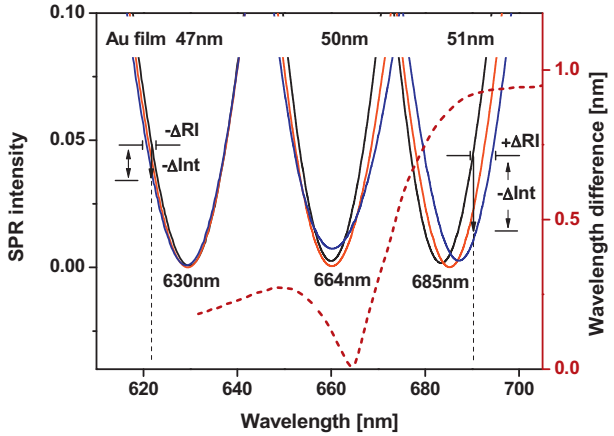

Fig. 4. Spectral SPR resonance curves obtained with optimal gold layer thicknesses 47 nm, 50 nm and 51 nm for surface plasmon excitation at 630 nm ($\lambda_{SPR} < \lambda_{max}$), 664 nm ($\lambda_{SPR} = \lambda_{max}$) and 685 nm ($\lambda_{SPR} > \lambda_{max}$) respectively. The calculations are performed for water (black), 0.1 mM (red) and 0.2 mM (blue) MB solutions. The principle for SPR intensity interrogation at 630 nm and 685 nm is presented. The spectral dependence of the absolute refractive index changes is shown as dotted line. (For interpretation of the references to color in this figure legend, the reader is referred to the web version of the article.)

In this article we have considered two types of absorptive redox mediator films that have been applied as sensing medium in eSPR sensors. Initially we investigated eSPR voltammograms for MB solution with different concentrations. Then, we applied eSPR spectroscopy to detect local redox reaction in the interfacial thin film created by stem-loop oligonucleotides with MB tags. Experimental eSPR voltammograms for 0.005, 0.05, 0.1 and 0.5 mM MB in PBS were obtained by cyclic potential scanning in the range of +0.1 to −0.5 V at 10 mV/s (Fig. 5). The wavelength difference correlated to the spectral resonance position at 0 V is presented on the *y*-axis and is directly related to variations in the real part of the refractive index. We estimated sensitivity of our spectral SPR at 2030 nm/RI at 664 nm. In Fig. 5A, we present eSPR results obtained at a 615 nm resonance wavelength, which is spectrally situated on the left shoulder of the oxidized MB absorption peak ($\lambda_{SPR} < \lambda_{max}$). eSPR voltammograms measured at 675 nm excitation wavelength are shown in Fig. 5B ($\lambda_{SPR} > \lambda_{max}$). The choice of these working wavelengths follows from the theoretically estimated maximal variation of the MB solution refractive index *n* (Fig. 2B). We observe rather different behaviors of the eSPR voltammograms for these two wavelengths. For example, when reduced at −0.5 V, the low 0.005 mM MB concentration demonstrates a positive wavelength shift at 615 nm (Fig. 5A, green) whereas at 685 nm, the wavelength shift is negative (Fig. 5B, green). These experimental results are in agreement with theoretical predictions for the RI difference as a function of wavelength (Fig. 2B). However, at 615 nm, even for 0.05 mM MB concentration, the voltage scan to −0.5 V already shows almost no RI changes. At higher MB concentrations,

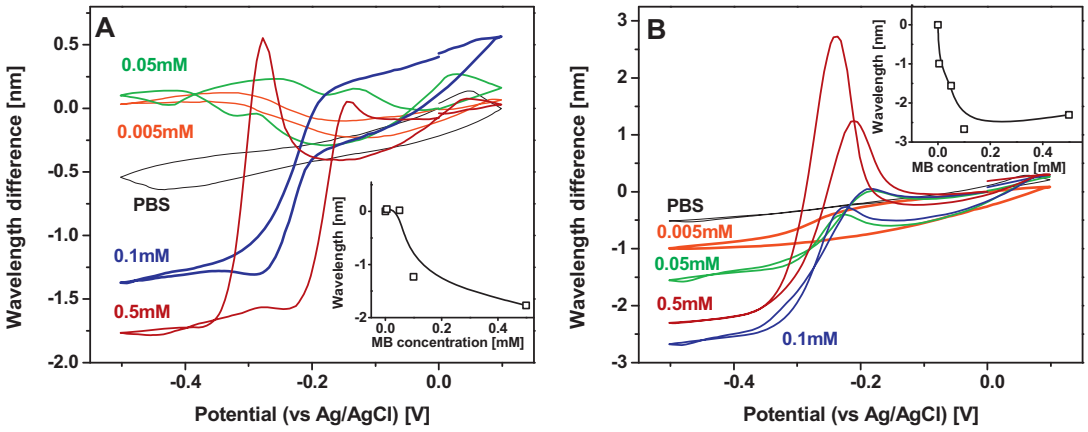

Fig. 5. Variations in the resonant SPR wavelength during cyclic voltammetry (10 mV/s, 100 mV to −500 mV) for various free MB concentrations. (A) Experimental results at λ_{SPR} = 615 nm, where the real part of the refractive index of the MB oxidized state is lower than the reduced state ($n_{ox} < n_{red}$). At low MB concentrations (0.005 and 0.05 mM), the SPR peak is shifted to lower wavelengths when oxidized in agreement with theory. At higher MB concentrations, the peak is shifted to higher wavelengths when oxidized. This is due to the competitive process of deposition of a thin MB layer on the surface. The peak observed at 0.5 mM is attributed to the dissolution of this MB thin film. (B) Experimental results at λ_{SPR} = 675 nm, where $n_{ox} > n_{red}$. At all MB concentrations, the resonant wavelength is shifted to higher wavelengths when oxidized in agreement with the theory. The same thin film deposition process is observed with a similar peak associated with dissolution at 0.5 mM. (For interpretation of the references to color in this figure legend, the reader is referred to the web version of the article.)

the negative potential induces a decrease in RI, which is in opposition with our theoretical predication that the RI will increase with MB concentration. The explanation lies in the fact that the negative potential applied to the working electrode generates two competitive processes. In addition to the MB reduction at −0.27 V, a thin film formed from positively charged oxidized MB molecules is formed at the interface and decreases the total measured RI. This effect is observed up to higher 0.5 mM MB concentration. We predict that these processes for eSPR sensing with 675 nm excitation will lead to increased RI at negative potentials for MB concentration equal and larger than 0.05 mM. However, it happens only for concentration larger than 0.1 mM. Explanation lies in the nonsymmetrical RI dependence around resonance 664 nm point (Fig. 2B). At 675 nm, reduction of MB will initiate absolute RI changes almost two times larger than at 615 nm due to existence of a second MB absorption peak at 615 nm. For MB in a solution with 0.5 mM concentration, we also observe additional positive peaks on the eSPR voltammograms related to the dissolution of the oxidized MB thin film. We can conclude that due to the complicated character of the eSPR measurement of the MB in the solution, multiple parameters have to be accurately considered for successful sensor realization. A careful choice of experimental eSPR parameters and sometimes multispectral detection will allow to correctly estimate measured effect and separate the RI changes due to MB reduction from the RI changes due to reversible MB thin film formation.

Uniform and stable redox mediator film with constant MB concentration for biosensing application can be created on the conducting interface by electropolymerization [30] or by functionalization with self-assembled monolayers or with redox-tagged DNA. In this article, stem-loop oligonucleotides with electrochemically active MB indicator were experimentally tested with spectral eSPR method (Fig. 1(II)). Electrochemical eSPR voltammograms for multiple spectral positions around MB absorption peak are presented in Fig. 6. As no diffusion processes are involved into MB electrochemical reduction-oxidation process experimental results for resonance eSPR peak position (Fig. 6A) and intensity variation (Fig. 6B) show very good agreement with absorption-based SPR principle for MB detection (Fig. 2B). In Fig. 7, we presented

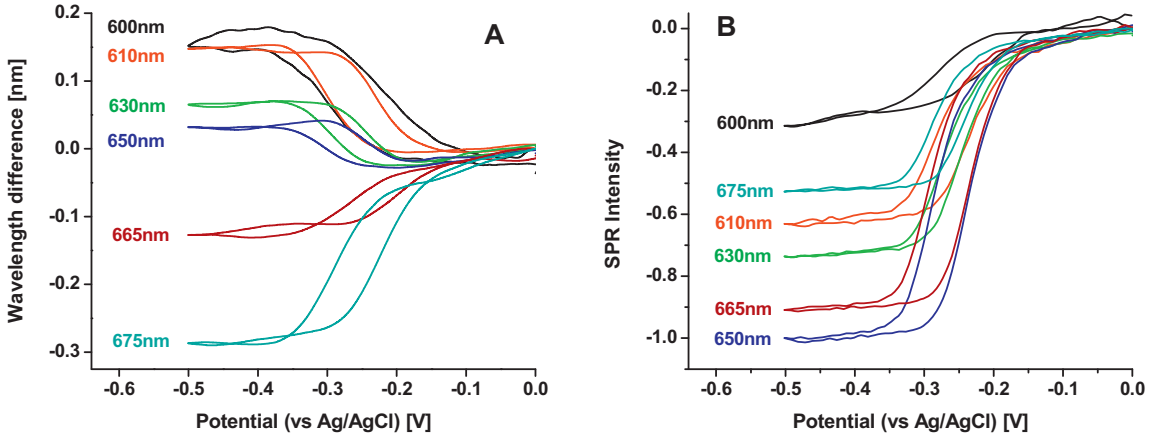

Fig. 6. Experimentals eSPR voltammograms showing the resonant SPR wavelength (λ_{SPR}) and intensity during cyclic voltammetry (10 mV/s, 0 mV to −500 mV) at various SPR resonant wavelengths for a surface modified with structure-switching sensor with MB indicator. (A) Variations in the resonant wavelengths as a function of applied potential. In accordance with Fig. 2, for $\lambda_{SPR} < \lambda_{max}$ (600, 610, 630, 650 nm), the absorbing oxidized state has a lower refractive index than the reduced state ($n_{ox} < n_{red}$) and the SPR peak is blue-shifted when oxidized. For $\lambda_{SPR} > \lambda_{max}$ (665 and 675 nm), $n_{ox} > n_{red}$ and the SPR peak is red-shifted when oxidized. (B) Variations in the SPR resonance peak intensity as a function of applied potential. The highest k difference, and therefore intensity contrast, between the oxidized and reduced states occurs around $\lambda_{SPR} = \lambda_{max}$ = 664 nm, as predicted in Fig. 2, and gradually decreases when λ_{SPR} departs from λ_{max}. (For interpretation of the references to color in this figure legend, the reader is referred to the web version of the article.)

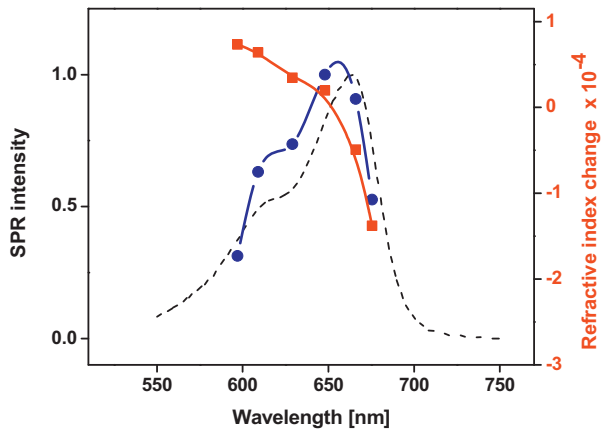

Fig. 7. Spectral dependences of electrochemically modulated SPR resonance peak intensity (blue) and effective medium RI (black solid line) as extracted from experimental data. Normalized MB absorption spectrum is shown in black dotted line for comparison. (For interpretation of the references to color in this figure legend, the reader is referred to the web version of the article.)

experimental spectral dependences for electrochemical variation of eSPR resonance peak intensity and effective medium RI changes in comparison with MB absorption spectrum (dotted line). We observe a good matching of experimental eSPR results with absorption characteristic of MB mediator film. Presented results could help to find optimal experimental conditions for electrochemical SPR sensing.

eSPR method allows for simultaneous SPR and electrochemical analysis of molecular binding processes and is less sensitive to bulk refractive index changes or nonspecific binding than conventional SPR. Its sensitivity and complexity of experimental realization depends on the choice of eSPR interrogation method. Real time detection of the SPR resonance peak position allows to reduce fluctuation in a light source and detector. Optimal experimental conditions include use of gold film thickness assuring minimum SPR reflection at $\lambda_{max} + \lambda_{1/2}$ resonance wavelength. However, eSPR intensity interrogation allows faster detection and compatibility with electrochemical impedance and AC voltammetry methods applied for reduction potential determination. Several choices of the optimal gold film thickness can be proposed (Fig. 3B). Gold film thickness dAu_0 with fixed excitation wavelength will generate intensity variation due to the real RI changes (Fig. 4, dotted lines). Two different gold film thickness values could be used to maximize absorption response of eSPR sensor (Fig. 3B). Whereas 68 nm layer will be more stable for simultaneous electrochemical experiments, using 36 nm provides larger SPR peak. It could simplify the optical setup alignment for correct incident angle-wavelength combination and allows using cheap LED light source with larger spectral range. Also, nonspecific attachments that shift the SPR resonance curve will have lower influence on the final eSPR results.

5. Conclusion

Complex behavior of the combined electrochemical and SPR biosensing technique applied to the analysis of the absorptive redox mediator film requires careful design of the experimental work and interpretation of the obtained results. The optimal eSPR system parameters are important to improve sensitivity and to find better interrogation method depending on the available technique and biosensing application. Methylene Blue electroactive redox tags show a good potential in the field of biosensors based on the detection of optical differences between reduced and oxidized species. Electrochemical MB modulation detected by eSPR methodology opens new possibilities in biosensor devices development by using all variety of plasmonic approaches from conventional propagating SPR to highly localized nanoplasmonic and nanoparticles based sensing.

References

[1] D.R. Walt, Ubiquitous sensors: when will they be here? ACS Nano 3 (2009) 2876–2880.
[2] H.X. Ju, J. Zhou, C.X. Cai, H.Y. Chen, The electrochemical behavior of methylene blue at a microcylinder carbon fiber electrode, Electroanalysis 7 (1995) 1165–1170.
[3] A. Erdem, K. Kerman, B. Meric, U.S. Akarca, M. Ozsoz, Novel hybridization indicator methylene blue for the electrochemical detection of short DNA sequences related to the hepatitis B virus, Anal. Chim. Acta 422 (2000) 139–149.
[4] A. Tani, A.J. Thomson, J.N. Butt, Methylene blue as an electrochemical discriminator of single- and double-stranded oligonucleotides immobilised on gold substrates, Analyst 126 (2001) 1756–1759.
[5] A. Vallee-Belisle, F. Ricci, T. Uzawa, F. Xia, K.W. Plaxco, Bioelectrochemical switches for the quantitative detection of antibodies directly in whole blood, J. Am. Chem. Soc. 134 (2012) 15197–15200.
[6] A.A. Lubin, R.Y. Lai, B.R. Baker, A.J. Heeger, K.W. Plaxco, Sequence-specific, electronic detection of oligonucleotides in blood, soil, and foodstuffs with the reagentless, reusable E-DNA sensor, Anal. Chem. 78 (2006) 5671–5677.
[7] B.M. Beam, N.R. Armstrong, S.B. Mendes, An electroactive fiber optic chip for spectroelectrochemical characterization of ultra-thin redox-active films, Analyst 134 (2009) 454–459.
[8] K. Imai, T. Okazaki, N. Hata, S. Taguchi, K. Sugawara, H. Kuramitz, Simultaneous multiselective spectroelectrochemical fiber-optic sensor: demonstration of the concept using methylene blue and ferrocyanide, Anal. Chem. 87 (2015) 2375–2382.
[9] A. Baba, M.K. Park, R.C. Advincula, W. Knoll, Simultaneous surface plasmon optical and electrochemical investigation of layer-by-layer self-assembled conducting ultrathin polymer films, Langmuir 18 (2002) 4648–4652.
[10] X.F. Kang, Y.D. Jin, G.J. Cheng, S.J. Dong, In situ analysis of electropolymerization of aniline by combined electrochemistry and surface plasmon resonance, Langmuir 18 (2002) 1713–1718.
[11] A. Baba, S.J. Tian, F. Stefani, C.J. Xia, Z.H. Wang, R.C. Advincula, et al., Electropolymerization and doping/dedoping properties of polyaniline thin films as studied by electrochemical-surface plasmon spectroscopy and by the quartz crystal microbalance, J. Electroanal. Chem. 562 (2004) 95–103.
[12] A. Baba, J. Lubben, K. Tamada, W. Knoll, Optical properties of ultrathin poly(3 4-ethylenedioxythiophene) films at several doping levels studied by in situ electrochemical surface plasmon resonance spectroscopy, Langmuir 19 (2003) 9058–9064.
[13] C. Li, T. Imae, Electrochemical and optical properties of the poly(3 4-ethylenedioxythiophene) film electropolymerized in an aqueous sodium dodecyl sulfate and lithium tetrafluoroborate medium, Macromolecules 37 (2004) 2411–2416.
[14] R. Georgiadis, K.A. Peterlinz, J.R. Rahn, A.W. Peterson, J.H. Grassi, Surface plasmon resonance spectroscopy as a probe of in-plane polymerization in monolayer organic conducting films, Langmuir 16 (2000) 6759–6762.
[15] Y. Iwasaki, T. Horiuchi, O. Niwa, Detection of electrochemical enzymatic reactions by surface plasmon resonance measurement, Anal. Chem. 73 (2001) 1595–1598.
[16] S. Sriwichai, A. Baba, S. Phanichphant, K. Shinbo, K. Kato, F. Kaneko, Electrochemically controlled surface plasmon resonance immunosensor for the detection of human immunoglobulin G on poly(3-aminobenzoic acid) ultrathin films, Sens. Actuators B: Chem. 147 (2010) 322–329.
[17] K. Nakamoto, R. Kurita, O. Niwa, One-chip biosensor for simultaneous disease marker/calibration substance measurement in human urine by electrochemical surface plasmon resonance method, Biosens. Bioelectron. 26 (2010) 1536–1542.
[18] X.F. Kang, G.J. Cheng, S.J. Dong, A novel electrochemical SPR biosensor, Electrochem. Commun. 3 (2001) 489–493.
[19] Y. Iwasaki, T. Horiuchi, M. Morita, O. Niwa, Analysis of electrochemical processes using surface plasmon resonance, Sens. Actuators B: Chem. 50 (1998) 145–148.
[20] J. Lu, W. Wang, S.P. Wang, X.N. Shan, J.H. Li, N.J. Tao, Plasmonic-based electrochemical impedance spectroscopy: application to molecular binding, Anal. Chem. 84 (2012) 327–333.
[21] X.N. Shan, S.P. Wang, W. Wang, N.J. Tao, Plasmonic-based imaging of local square wave voltammetry, Anal. Chem. 83 (2011) 7394–7399.
[22] X.N. Shan, U. Patel, S.P. Wang, R. Iglesias, N.J. Tao, Imaging local electrochemical current via surface plasmon resonance, Science 327 (2010) 1363–1366.
[23] A.M. Dallaire, S. Patskovsky, A. Vallee-Belisle, M. Meunier, Electrochemical plasmonic sensing system for highly selective multiplexed detection of biomolecules based on redox nanoswitches, Biosens. Bioelectron. 71 (2015) 75–81.

[24] K. Kurihara, K. Suzuki, Theoretical understanding of an absorption-based surface plasmon resonance sensor based on Kretchmann's theory, Anal. Chem. 74 (2002) 696–701.
[25] E. Fujii, T. Koike, K. Nakamura, S. Sasaki, K. Kurihara, D. Citterio, et al., Application of an absorption-based surface plasmon resonance principle to the development of SPR ammonium ion and enzyme sensors, Anal. Chem. 74 (2002) 6106–6110.
[26] E. Fu, S.A. Ramsey, J. Chen, T.M. Chinowsky, B. Wiley, Y. Xia, et al., Resonance wavelength-dependent signal of absorptive particles in surface plasmon resonance-based detection, Sens. Actuators B: Chem. 123 (2007) 606–613.
[27] H. Kano, S. Kawata, Surface-plasmon sensor for absorption-sensitivity enhancement, Appl. Opt. 33 (1994) 5166–5170.
[28] A.B. Dahlin, J.O. Tegenfeldt, F. Hook, Improving the instrumental resolution of sensors based on localized surface plasmon resonance, Anal. Chem. 78 (2006) 4416–4423.
[29] K. Bergmann, C. O'konski, A spectroscopic study of methylene blue monomer, dimer, and complexes with montmorillonite, J. Phys. Chem. 67 (1963) 2169–2177.
[30] K.C. Lin, C.Y. Yin, S.M. Chen, An electrochemical biosensor for determination of hydrogen peroxide using nanocomposite of poly(methylene blue) and FAD hybrid film, Sens. Actuators B: Chem. 157 (2011) 202–210.

Biographies

Sergiy Patskovsky received his B.S. degree in Radiophysics Faculty from Taras Shevchenko University of Kiev in 1986 and his Ph.D. degree from Polytechnique Montréal in 2005, where he is currently a Research Associate at Engineering Physics Department. His research mainly focuses on plasmonic biosensing, biophotonics and hyperspectral optical imaging.

Anne-Marie Dallaire received her B.Ing. and M.Sc.A. in engineering physics from Polytechnique Montréal in 2013 and 2015, respectively. Her research mainly focuses on the development and characterization of combined electrochemical and surface plasmon resonance biosensors applied for the detection of DNA and biomolecules in crude samples.

Michel Meunier received his B.Ing. and M.Sc.A. degrees in engineering physics from Polytechnique Montréal in 1978 and 1980, respectively, and his Ph.D. degree from the Massachusetts Institute of Technology in 1984. He is currently the Director of the Laser Processing and Plasmonics Laboratory at Polytechnique Montréal. For 33 years, he has been involved in laser processing of various materials and biological applications, and he has published over 330 papers in this field. He is a Fellow of the SPIE, OSA and the Canadian Academy of Engineering. He holds a Canadian Research Chair in laser micro/nanoengineering of materials.